



10 – 12 may, Aveiro, Portugal

**SiF'06**

## Fourth International Workshop Structures in Fire

Taken from the proceedings page 139 - 150

### **LIGHT WEIGHT STRUCTURES EXPOSED TO FIRE: A STAINLESS STEEL SANDWICH PANEL**

PETER SCHAUMANN<sup>1</sup>, TIINA ALA-OUTINEN<sup>2</sup>,  
FLORIAN KETTNER<sup>3</sup> and OLLI KAITILA<sup>4</sup>

#### ABSTRACT

A new type of laser-welded stainless steel sandwich panel with rock wool insulation has been developed by Kenno Tech Ltd. It is the aim of the present study, conducted in the frame of the RFCS project “Stainless Steel in Fire”, to prove that a fire resistance of 30 to 60 minutes can be achieved without additional active or passive fire protection. The sandwich panel system has been tested in small and large scale fire tests to investigate the thermal and load bearing behaviour of the element exposed to fire. Furthermore, numerical models have been established. This contribution focuses on the presentation of the thermal and mechanical numerical analysis, which were performed with the general purpose FE-software packages *ABAQUS/Standard* and *COMSOL Multiphysics*. As the mechanical response of the structural element has no influence on the heating of the member, the thermal and mechanical problems could be solved separately. Thermal analysis have been performed in 2D with *ABAQUS/Standard* and *COMSOL Multiphysics* considering material nonlinearities. The results of the two programs are compared to each other and to the test results. The mechanical analysis was performed with *ABAQUS/Standard* using a three-dimensional shell model and considering material nonlinearities, buckling analysis and the effect of high temperatures on the structural behaviour. The results are compared to fire tests.

---

1 Professor, University of Hannover, Institute for Steel Construction, Appelstr. 9a, 30167 Hannover, Germany  
email: [schaumann@stahl.uni-hannover.de](mailto:schaumann@stahl.uni-hannover.de)

2 M.Sc. (Tech.), VTT Technical Research Centre of Finland, P.O. Box 1000, FI-02044 VTT, Finland  
email: [tiina.ala-outinen@vtt.fi](mailto:tiina.ala-outinen@vtt.fi)

3 Research Assistant, University of Hannover, Institute for Steel Construction, Appelstr. 9a, 30167 Hannover, Germany, email: [kettner@stahl.uni-hannover.de](mailto:kettner@stahl.uni-hannover.de)

4 D.Sc. (Tech.), VTT Technical Research Centre of Finland, P.O. Box 1000, FI-02044 VTT, Finland  
email: [olli.kaitila@vtt.fi](mailto:olli.kaitila@vtt.fi)

## 1. INTRODUCTION

The RFSC-project (Contract No RFS-CR-04048) “Stainless Steel in Fire” seeks to develop more comprehensive and economic design guidance on structural stainless steel members and connections in fire. This includes specific unprotected products meeting the requirements for 30 and 60 minutes fire resistance. The project covers tests on materials, members and connections, numerical analysis and development of design guidance. The comprehensive final report will provide design guidance in a suitable format for inclusion in European standards, accompanied by web-based design software.

This paper deals with a new type of laser-welded stainless steel sandwich panel developed by Kenno Tech Ltd. and analysed in the frame of the project. The sandwich panel consists of two stainless steel sheets as cover plates and V-profiles comprising the web of the section, as shown in Fig. 1. The voids are filled with insulation material, e.g. rock wool, to improve the thermal behaviour. It is the aim of the study to prove that a fire resistance of 30 to 60 minutes can be achieved without additional active or passive fire protection.



Fig. 1 – Stainless steel sandwich panel.

The main structural benefit of this type of welded metal sandwich panels is a high strength to weight ratio, which means advantages for transport and installation at the building site. Previously, these types of structures have been made of carbon steel, but new welding techniques have made it possible to produce them also from stainless steel. The main applications for the sandwich panels are in transportation, ship building, construction industry and process industry, especially where the advantages of stainless steel (resistance to corrosion, increased strength in fire situation, sanitary applications, low maintenance costs) can be beneficial.

## 2. STRUCTURAL FIRE TESTS

An unloaded small scale and a loaded large scale test have been carried out at the VTT Fire Research testing laboratory on the corrugated core sandwich panels with rock wool insulation fabricated by the Finnish company Kenno Tech Ltd. The dimensions of the specimens were decided on the basis of computed results and are shown in Fig. 4. The total thickness of the sandwich panels was 124.5 mm and the stainless steel grade was EN 1.4301. The spaces between the core elements were filled with blowing rock wool with a density of  $115 \text{ kg/m}^3$ , calculated on the basis of the small scale test specimen. The thermal action followed the EN 1363-1: 1999<sup>1</sup> (ISO 834-1) standard fire curve. The temperatures measured by furnace thermocouples were averaged automatically, and the average was used for controlling the furnace temperature. Temperature readings were taken at each thermocouple at intervals of 10 s.

The small scale test was carried out in the cubic furnace on a specimen with horizontal dimensions equal to approximately  $1250 \times 1250 \text{ mm}$ . The element was installed onto the top opening of the furnace so that its bottom surface was exposed to heating and the top surface was open to the testing hall.

The cross-section of the insulated floor construction in the large scale test was similar to that in the small scale test. The floor consisted of two equal panels with a seam in the middle. The width of one full panel was 1504 mm, the length 5405 mm and the thickness 125 mm. The total width of the furnace ceiling was 3015 mm. The test specimen was loaded during the test. The calculated variable action at normal temperature was  $250 \text{ kg/m}^2$  and in the fire situation 50 % of that. The elements were installed onto the top opening of the furnace so that their bottom surfaces were exposed to heating. The top surface was covered with an 11 mm thick and 2708 mm wide chipboard. The seam between the panels was protected with a stainless steel casing and rock wool insulation attached from underneath, as shown in Fig. 2.

Unfortunately, the installation of the blowing rock wool was not successful for the large scale test specimen and there were several areas of very low insulation density. This caused scatter in the temperature measurements and the failure of the specimen in terms of fire separating function at a relatively early stage.

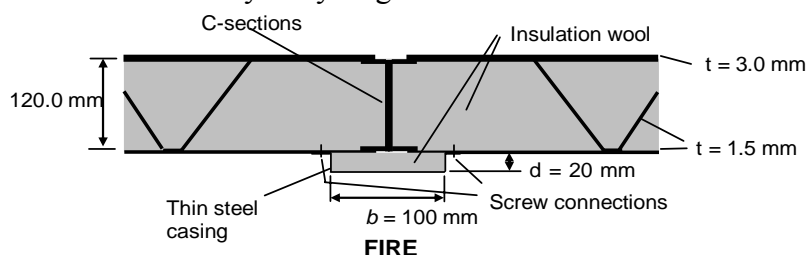


Fig. 2 – Cross-section of test specimens showing seam between floor panels in large scale test.



Fig. 3 – Large scale test setup: furnace (left) and applied variable loads (right).

### 3. MATERIAL MODELS

#### 3.1 Thermal material properties

The thermal properties of stainless steel were determined according to EN 1993-1-2<sup>2</sup>. The thermal properties of the blowing rock wool used in the tests were not directly available. Models for rock wool slabs of densities  $30 \text{ kg/m}^3$  (wool30) and  $140 \text{ kg/m}^3$  (wool140) had been determined by VTT on the basis of earlier tests, so these were expected to provide upper and lower bounds for the temperature calculations. The specific heat capacities  $c$  for wool30 and wool140 were taken as  $900 \text{ J/kgK}$  and  $800 \text{ J/kgK}$ , respectively. The thermal conductivities  $\lambda$  (W/mK) were modelled according to Eq. (1) for wool30 and Eq. (2) for wool140, where  $T$  is the insulation temperature ( $^{\circ}\text{C}$ ).

$$\lambda = 0.034 - 0.00016T + 1.09 \cdot 10^{-6}T^2 \quad (1)$$

$$\lambda = 0.0341 - 0.0095(T/100) + 0.0034(T/100)^2 \quad (2)$$

### 3.2 Mechanical material properties for stainless steel

A model for the mechanical material properties for stainless steel at elevated temperatures can be obtained from EN 1993-1-2<sup>2</sup>, where the stress is given as a function of strain, temperature and alloy. The general formulation for the stress-strain relationship is shown on the left in Fig. 4 and it is evaluated at different material temperatures on the right.

Stainless steel has no distinctive yield stress in comparison to conventional structural steel and consequently no horizontal plateau but is given as continuously increasing function as shown in Fig. 4. For steel with no yield plateau the nominal strength value is defined by the proof stress at 0.2 % plastic strain  $f_{0.2p}$ .

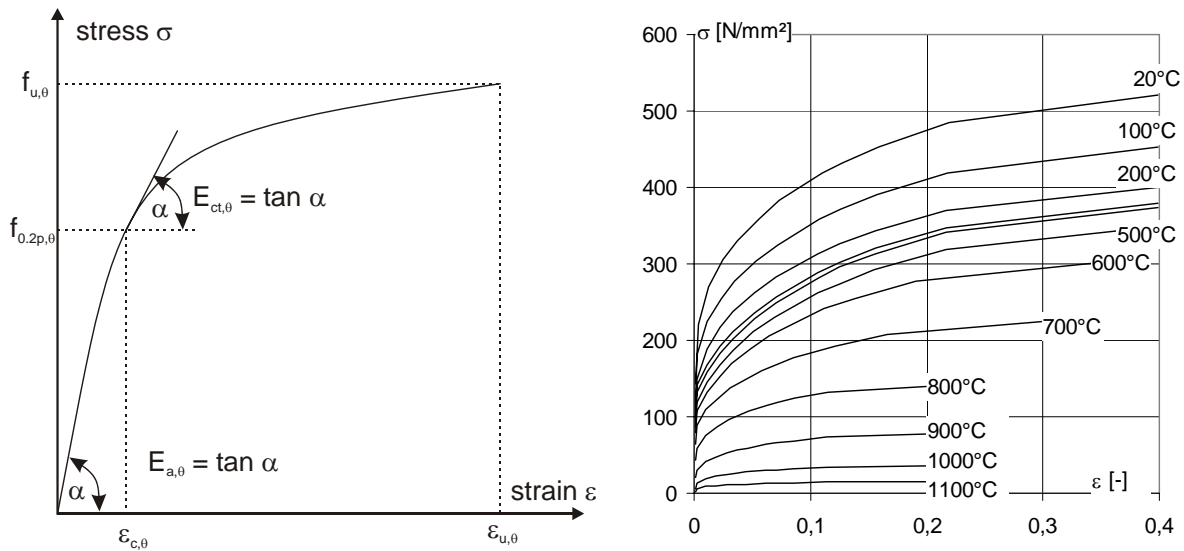


Fig. 4 – General stress-strain formulation (left) and evaluation at different temperatures (right) for stainless steel EN 1.4301 according to EN 1993-1-2.

For the numerical studies in *ABAQUS*, true stresses and logarithmic strains were used as given in Eq. (3) and Eq. (4), respectively.

$$\sigma_{true} = \sigma_{nom} (1 + \epsilon_{nom}) \quad (3)$$

$$\epsilon_{ln}^{pl} = \ln(1 + \epsilon_{nom}) - \frac{\sigma_{true}}{E} \quad (4)$$

Furthermore, EN 1993-1-2<sup>2</sup> gives an approach for the thermal elongation according to Eq. (5), but for the use in *ABAQUS*, a constant thermal expansion coefficient was derived from Eq. (5), as given in Eq. (6).

$$\Delta L/L = (16 + 4.79 \cdot 10^{-3} \theta_a - 1.243 \cdot 10^{-6} \theta_a^2) \cdot (\theta_a - 20) \cdot 10^{-6} \quad (5)$$

$$\alpha_\theta = \frac{d(\Delta L/L)}{d\theta} \approx 1.8 \cdot 10^{-5} \quad (6)$$

## 4. THERMAL FE-MODELLING

### 4.1 General model information

The thermal analysis for the floor slab was done using *COMSOL Multiphysics*<sup>3</sup> and *ABAQUS/Standard*<sup>4</sup> with two-dimensional incremental temperature calculation of the cross section using the Finite Element Method. The two models are illustrated in Fig. 5. In *ABAQUS*, only a small part of the cross section was modelled in order to improve efficiency by taking advantage of symmetry conditions. In *COMSOL*, a larger cross-section could be modelled without problems due to high calculation times.

Three- and four-node elements with linear shape functions were used in *ABAQUS* for the implementation of the stainless steel parts and the rock wool including direct heat flux between the two materials. In *COMSOL*, the meshing is done automatically by the program using triangular linear elements. The thermal boundary conditions were taken as adiabatic at symmetry boundaries for both models. The thermal action on the bottom surface of the slab was modelled according to the standard temperature-time curve as defined in EN 1363-1: 1999<sup>1</sup> (ISO 834-1) with convective and radiative heat transfer ( $\alpha_c = 25 \text{ W}/(\text{m}^2\text{K})$ ;  $\varepsilon_{res} = 0.2$  in *ABAQUS* and  $\varepsilon_{res} = 0.4$  in *COMSOL*). On the unexposed (top) surface of the slab, the heat loss was implemented with a constant ambient temperature of 20°C and convective heat transfer with  $\alpha_c = 9 \text{ W}/(\text{m}^2\text{K})$  in *ABAQUS* and  $\alpha_c = 4 \text{ W}/(\text{m}^2\text{K})$  in *COMSOL*. Additionally, radiation heat transfer from the unexposed surface to the ambient was considered in *COMSOL* with an emissivity of  $\varepsilon_{res} = 0.4$  (EN 1991-1-2: 2002<sup>5</sup>). Fig. 5 also shows temperature plots at analysis times of 30 and 60 minutes.

Because a material model for the blowing rock wool used in the tests was not available, the calculation was performed with rock wools of density  $\rho = 30 \text{ kg}/\text{m}^3$  (wool30) and  $\rho = 140 \text{ kg}/\text{m}^3$  (wool140). The application of the low density rock wool 30 led to slower heat flux in the area of the web than in the area of pure rock wool. This phenomenon can be explained by the thermal diffusivity  $a$ , which is defined in Eq. (7)

$$a = \frac{\lambda}{c \cdot \rho} \quad \left[ \frac{\text{mm}^2}{\text{s}} \right] \quad (7)$$

The thermal diffusivity defines the diffusion of heat in a medium and depends on thermal conductivity  $\lambda$ , which is higher for steel than for the insulation material, as well as on density  $\rho$  and thermal capacity  $c$ . The thermal diffusivity is plotted in Fig. 6 as a function of the material temperature for stainless steel and two different rock wools. The comparison demonstrates that for temperatures higher than 400°C, the values for wool30 are higher than the values for stainless steel and high density rock wool, which leads to the effect shown on the right in Fig. 6.

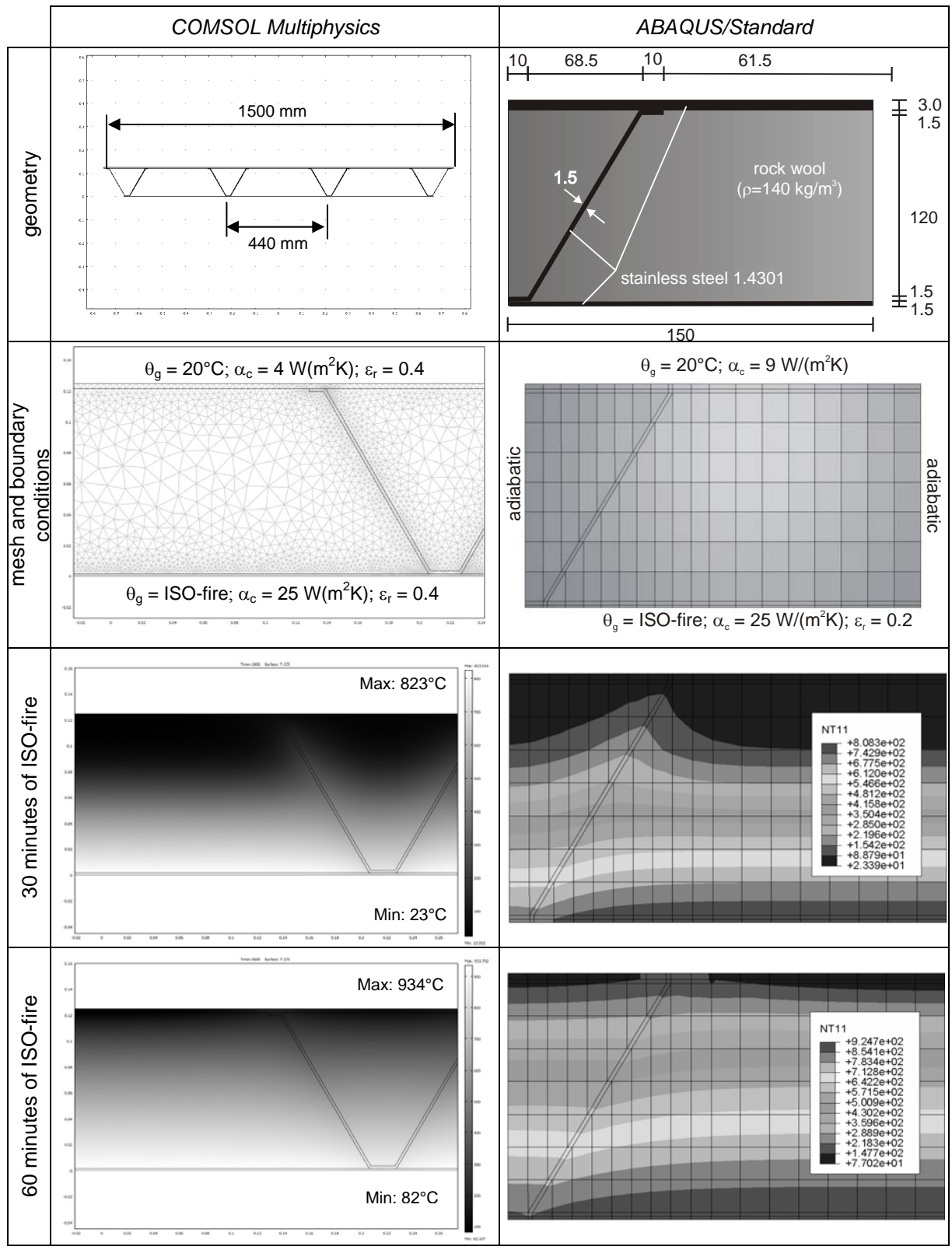


Fig. 5 – Thermal modelling in COMSOL and ABAQUS.

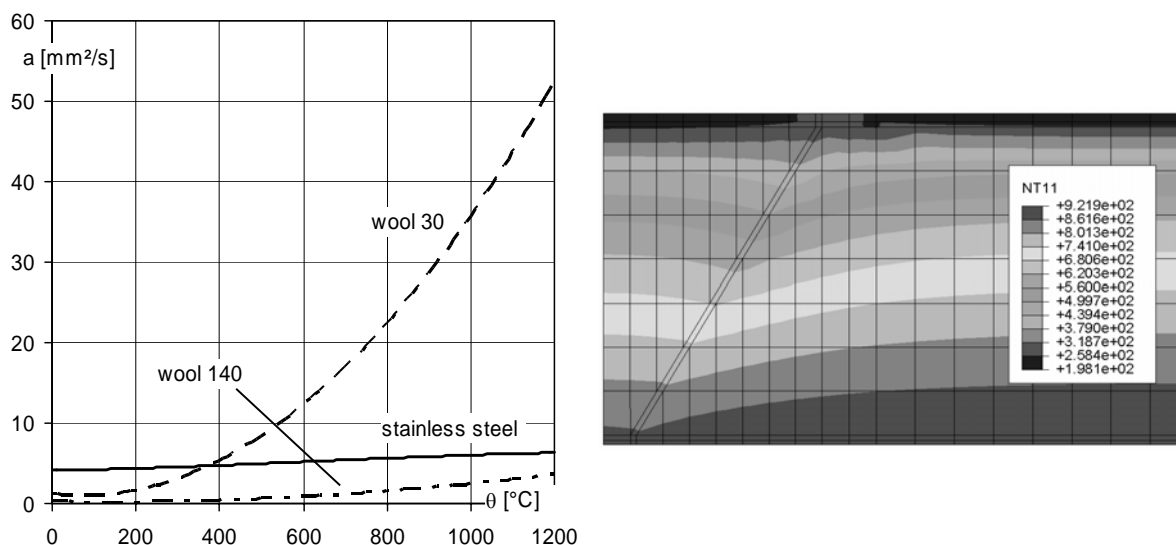


Fig. 6 – Thermal diffusivity of stainless steel, rock wool 30 and 140 (left) and temperature distribution after 30 minutes ISO-fire with rock wool 30 (right).

#### 4.2 Comparisons between numerical calculations and measured temperatures

The results of the numerical analysis using *COMSOL* and *ABAQUS* were compared with the measured temperatures of the small and large scale fire tests and are illustrated in Fig. 7. The temperatures are divided in three diagrams: for the upper flange of the steel profile (unexposed side), the middle of the web and the lower sheet (exposed side). All measured values that refer to the same part of the cross section (e.g. lower sheet), but are disposed over the area of the test specimen, are plotted in small dotted lines. An average value was calculated from these measured values and is shown as a thick line. The results of the numerical calculations are plotted for rock wool 30 and 140.

For the small scale test, the comparisons show that the numerical calculations are conservative in relation to the average values of the measured temperatures. Furthermore, the results with high density rock wool lie closer to the measured values of the small scale test. Unfortunately, due to the problems in blowing rock wool installation, there is a lot of scatter in the results of the large scale test. This makes comparisons with calculations difficult and these results should be considered with caution. However, fairly good agreement between *ABAQUS* and *COMSOL* analysis results can be seen here as well.

When comparing the average temperatures of small and large scale tests, it is obvious that the temperatures at the unexposed side are about 100 % higher in the large scale test, while the temperatures at the exposed side are nearly the same. These circumstances lead to different temperature gradients over the height of the member and this will be significant regarding the deflection (rf. section 5.3).

The Eurocodes define insulation criteria for separating members: the temperature at the unexposed side of the member must not exceed  $140^\circ\text{C}$  as average and  $180^\circ\text{C}$  as peak value. The measured temperature results reveal that the insulation criterion I 60 is met in the small but not in the large scale test.

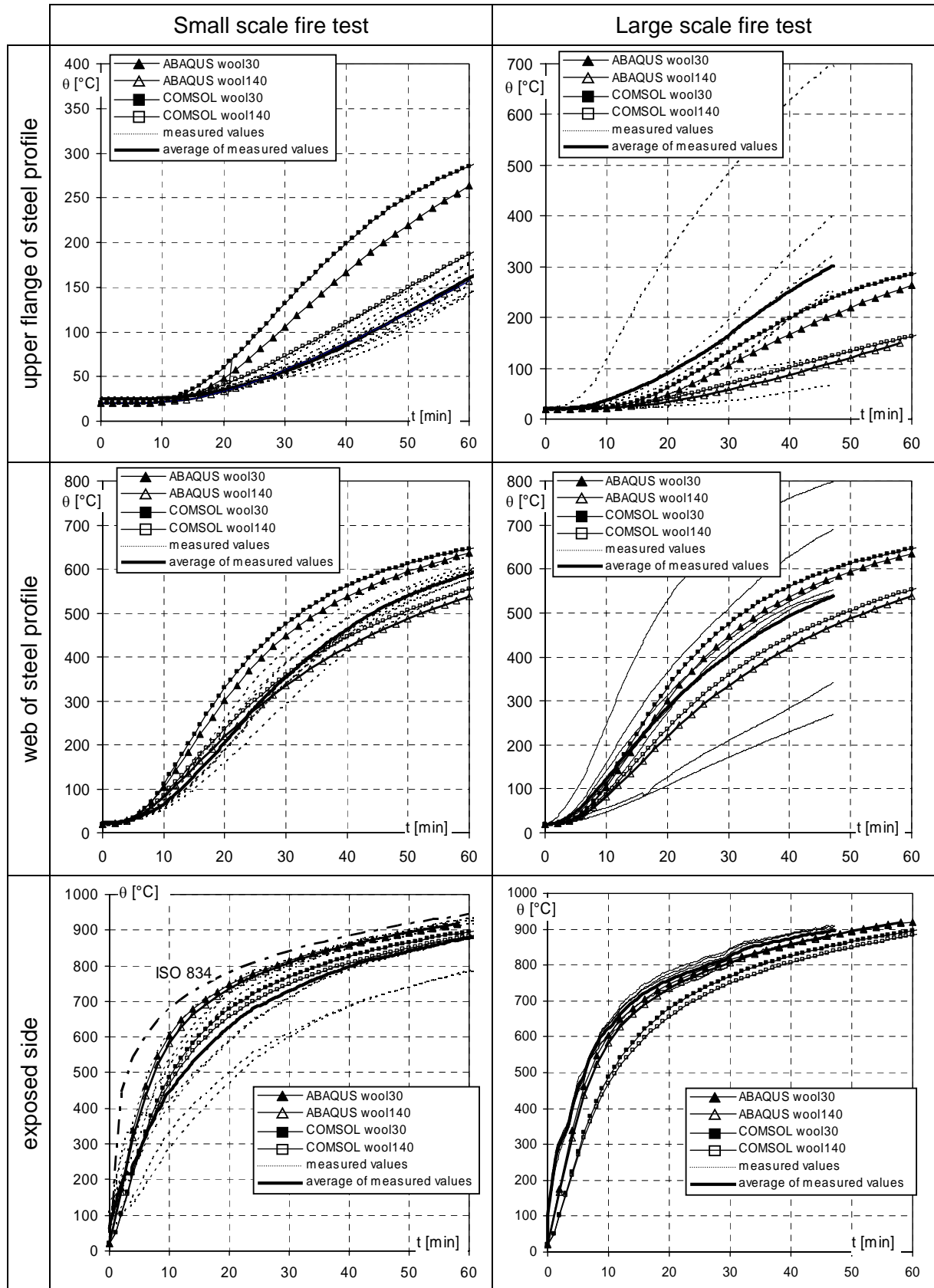


Fig. 7 – Comparisons between numerical calculations and measured temperatures from fire tests.

## 5. MECHANICAL FE-MODELLING

### 5.1 ABAQUS-model

A three-dimensional *ABAQUS*-model was set up for a load bearing calculation using S4R shell elements with reduced integration. Only a small part of the test specimen was implemented to reduce the size of the model and hence the required calculation time. The model represents one half of a rib, because the V-profiles of the floor element cause a one-way spanning load bearing behaviour so that the load-carrying in transverse direction is negligible. The boundary conditions were applied as shown in Fig. 8.

The numerical studies were performed in five steps:

1. Identification of buckling modes by linear buckling analysis to determine imperfections
2. Application of the imperfect geometry obtained in step 1
3. Application of mechanical loads
4. The loaded sandwich panel is subjected to the heating according to the small scale fire test
5. Load increasing with constant temperature distribution of 60 minutes of ISO-fire

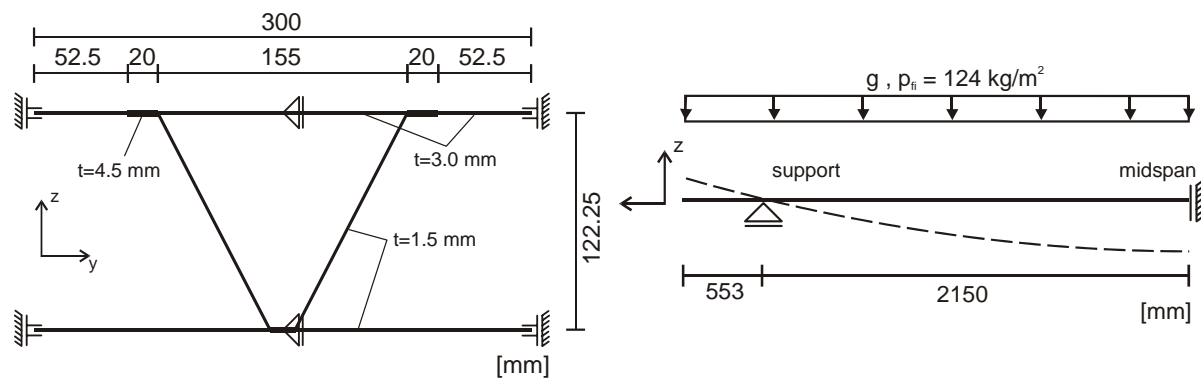


Fig. 8 – Geometry and boundary conditions of the ABAQUS-model: continuous boundary conditions along the edges (left) and at the ends of the rib (right).

### 5.2 Determination of imperfections – Linear buckling analysis

For a realistic estimation of the load bearing capacity, geometric imperfections must be considered in the analysis. The imperfections are simulated by superposing the FE-model with scaled buckling mode shapes determined in a linear buckling analysis with a basic state considering vertical loading, material nonlinearities and different temperature fields. The comparison of the different basic states revealed that the magnitude of the eigenvalues differed, but not the buckling shape. Finally, the imperfection has been developed from a superposition of two buckling modes, which are presented in Fig. 9: one for the compression zone in the upper flange at midspan and the other for the compression zone at the support. A common maximum magnitude for the imperfections was applied according to Eq. (8). The buckling mode shape according to Fig. 9 is scaled with  $\omega$  and superposed with the perfect geometry.

$$\omega = b / 200 = 155.0 / 200.0 = 0.775 \text{ mm} \quad (8)$$

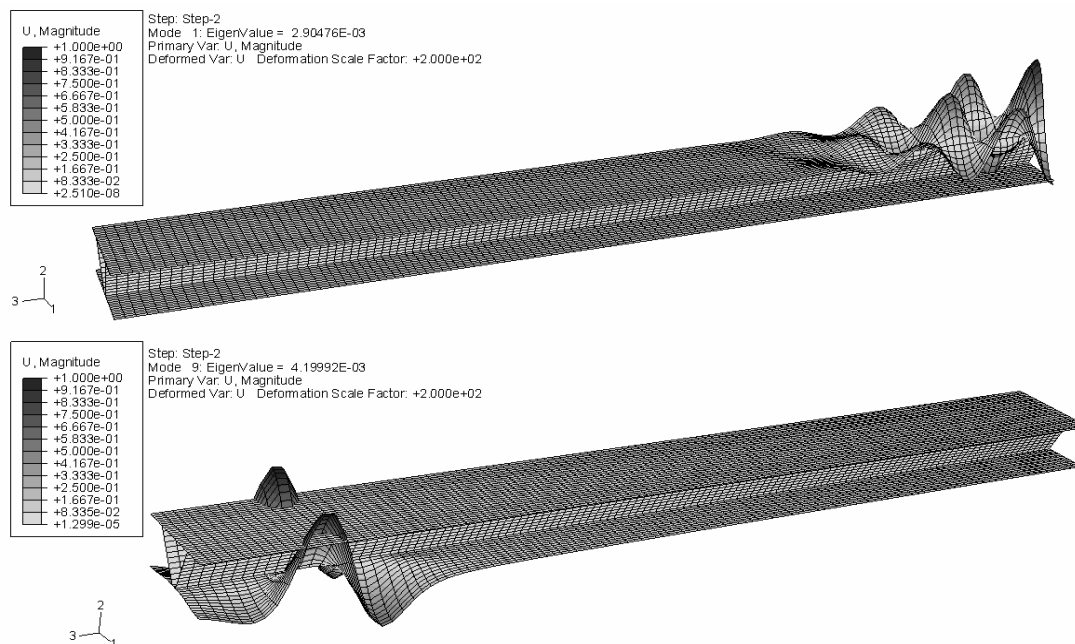


Fig. 9 – Buckling modes for the two compression zones at midspan and at support.

### 5.3 Load bearing behaviour of the sandwich panel subjected to ISO-fire

Finally, the sandwich panel with the imperfect geometry was subjected to the temperatures determined in the small scale fire test (rf. section 2). The analysis procedure is described in 5.1. The deformed shape is presented in Fig. 10 with a contour-plot showing Mises-stresses after 60 minutes of ISO-fire. Further investigation of the strains showed that no significant plastification occurred.

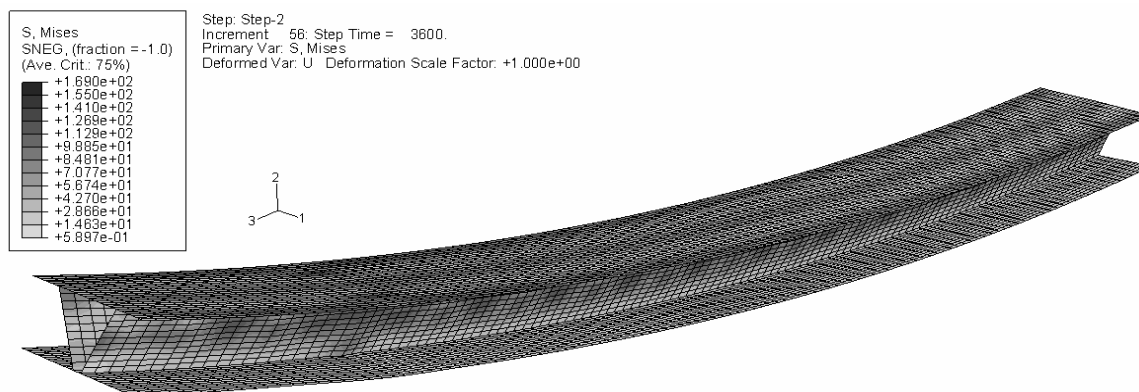


Fig. 10 – Deformed *ABAQUS*-model and Mises-stresses after 60 minutes of ISO-fire (no amplification).

The nodes at midspan and at the end of the cantilever arm at the lower sheet in the middle of the two webs were chosen as reference nodes for the time-displacement curve in Fig. 11. In addition to vertical deflections resulting from the external loading, thermal bowing determined according to simplified equations for the deflection midspan Eq. (9) and at the end of the cantilever arm Eq. (10) is depicted in Fig. 11.

$$w_{\theta,m} = \frac{L^2}{8} \alpha_T \frac{\Delta\theta}{d} \quad (9)$$

$$w_{\theta,c} = \frac{L_c}{2} \alpha_T \frac{\Delta\theta}{d} \cdot (L + L_c) \quad (10)$$

where  $d$  distance of the upper and lower flange  
 $\Delta\theta$  temperature gradient  
 $\alpha_T$  expansion coefficient  
 $L$  span between supports  
 $L_c$  span of the cantilever arm

The comparisons in Fig. 11 (left) between measured values and the results of the *ABAQUS* analysis show significant differences for the deflection at midspan  $w_m$ . The deflection governed by thermal bowing, as derived from Eq. (9) and (10) is also plotted in Fig. 11. Obviously, the total deflection during 60 minutes of ISO-fire in *ABAQUS* is governed by thermal bowing, and not by the effects of the mechanical loads and the loss in bending stiffness due to high steel temperatures. The reason for the differences between the test and the numerical analysis is the application of small scale fire test temperatures on the numerical model, because those values differ from the temperatures measured in the large scale test (see Fig. 7). Therefore the thermal bowing determined from the large scale temperatures are plotted in Fig. 11 as well. The maximum deflection thus obtained fits well with measured values of the large scale test.

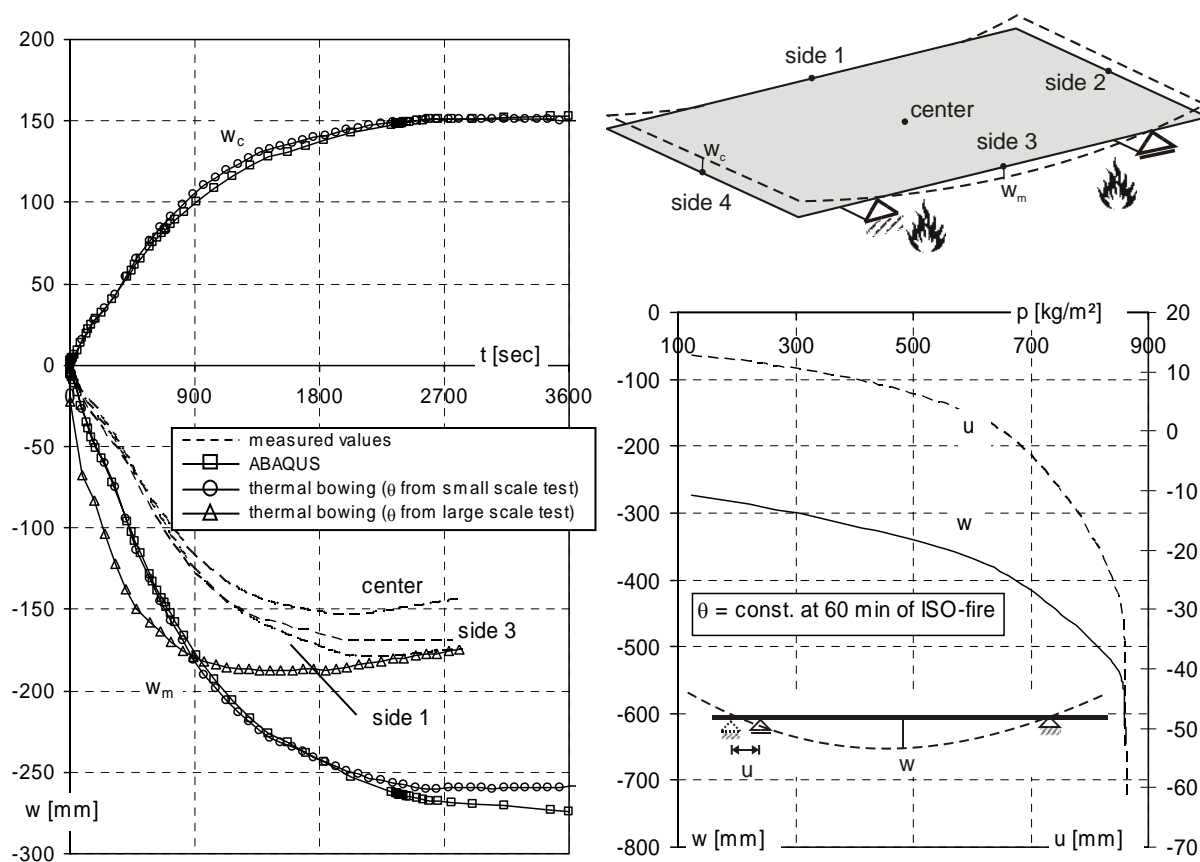


Fig. 11 – Deflections at various points (left) against time and vertical and horizontal displacements at midspan and at support against loads at constant temperatures of 60 min ISO-fire (right).

Overall, the deflections show that the requested fire resistance of 60 min for load bearing capacity was reached and failure did not occur. For this reason, a load bearing calculation was performed following the heating of 60 minutes of ISO-fire with constant temperatures and increasing live loads. The results for the deflection at midspan and the horizontal displacement at support are plotted on the right side of Fig. 11. An ultimate load  $p \approx 800 \text{ kg/m}^2$  for the structural member can be estimated from the graphs for R 60 due to rapidly increasing deflections. However, the large deflections due to thermal bowing may define a lower limit state for serviceability.

## 6. SUMMARY AND CONCLUSIONS

This contribution presented a new type of laser-welded stainless steel sandwich panel with rock wool insulation developed by Kenno Tech Ltd. and analysed in the frame of the RFCS-project “Stainless Steel in Fire”. Two fire tests have been performed with the element subjected to ISO-fire: an unloaded small scale test to analyse the temperature development and a large scale test with additional live load. Numerical and test results on the thermal and load bearing behaviour were demonstrated and explained.

Two-dimensional thermal analyses were performed using commercial FEM-software packages *COMSOL Multiphysics* and *ABAQUS/Standard*. The thermal analysis results from the two FEM-codes showed good agreement with each other and with the average values of the measured temperatures from the small scale test. However, the temperatures of the large scale test scatter because the installation of the blowing rock wool was not successful for the test specimen and there were several areas of very low insulation density.

A three-dimensional shell model has been set up in *ABAQUS* for the investigation of the load bearing behaviour of the panel. The model considered imperfections determined from linear buckling analysis, non-linear material behaviour of stainless steel and large deformations. The results demonstrated that the requested fire resistance of 60 min for load bearing capacity was reached and failure did not occur. However, the deflections up to 60 minutes of ISO-fire action were mainly governed by thermal bowing, not by the effects of the mechanical loads and the loss in bending stiffness due to high steel temperatures. Furthermore, the deflections determined using *ABAQUS* were obviously higher than in the large scale test. The reason was that in *ABAQUS*, the temperatures of the small scale test were applied on the structural model and the upper sheet in the large scale test shows higher temperatures than in the small scale test due to the insulation cavities. Thus the large scale test specimen had a smaller temperature gradient and hence smaller deflections due to thermal bowing.

Furthermore, the live load on the *ABAQUS*-model was continuously increased until failure could be observed due to rapidly increasing deflections.

## REFERENCES

- [1] EN 1363-1: 1999 *Fire resistance tests – Part 1: General requirements*, CEN European Committee for Standardization, Brussels, Belgium, 1999.
- [2] EN 1993-1-2 *Eurocode 3: Design of steel structures - Part 1.2: General rules, Structural fire design*, CEN European Committee for Standardization, Brussels, Belgium, 2005.
- [3] COMSOL Multiphysics© Version 3.2, *User's Guide*, COMSOL AB, 2005
- [4] ABAQUS/Standard© Version 6.5-1, *User's Manual*, ABACOM Software, 2004
- [5] EN 1991-1-2: 2002 *Eurocode 1 Actions on structures - Part 1-2: General actions - Actions on structures exposed to fire*, CEN European Committee for Standardization, Brussels, Belgium, 2002.